

The effects of ligand substitution and deuteration on the spectroscopic and photophysical properties of $[\text{Ru(LL)(CN)}_4]^{2-}$ complexes.

Margit Kovács,^a Kate L. Ronayne,^b Wesley R. Browne,^{c,d} William Henry,^c Johannes G. Vos,^c John J. McGarvey,^b and Attila Horváth^{*a}

Analytical data for ligands and complexes.

[D₂]-4,7-diphenyl-1,10-phenanthroline: Mass spectrometry HM⁺ ion at 335 m/z. ¹H NMR in [D₃]-chloroform δ ppm; 9.36 (H2/9, *resid.* s), 7.70 (H3/8, s), 7.64 (phenyl-4,7, m), 7.96 (H5/6, s). ²D NMR in [H₆]-acetone δ ppm; 9.2 (D2/9)

[D₁₂]-4,7-diphenyl-1,10-phenanthroline: Mass spectrometry HM⁺ ion at 347 m/z. ¹H NMR in [D₃]-chloroform δ ppm ; 9.36 (H2/9, s), 7.70 (H3/8, *resid.* s), 7.64 (phenyl-4,7, *resid.* s), 7.96 (H5/6, s). ²D NMR in [H₆]-acetone δ ppm; 7.91 (D3/8), 7.63 (phenyl-4/7, *resid.* D5/6)

K₂[Ru([D₈]-bpy)(CN)₄].2H₂O (**1b**): Yield 25%. Abs 284 nm ($\pi-\pi^*$), 400 nm (MLCT); Corrected emission maximum: 621 nm (298 K); ²H NMR (H₂O, 293 K) 9.13, 8.18, 7.91, 7.46; IR v(CN), 2036, 2045, 2058, 2093 cm⁻¹,

K₂[Ru([D₁₂]-dmb)(CN)₄].2H₂O (**2b**): Yield 20 %. Abs 283 nm ($\pi-\pi^*$), 393 nm (MLCT); Corrected emission maximum: 615 nm (298 K); ¹H NMR (D₂O): δ 8.95 (*resid.* s), 7.89 (*resid.* s), 7.24 (*resid.* s), 2.21 (*resid.* broad s), ²H NMR (H₂O, 293 K): δ 8.92, 7.94, 7.28, 2.24; IR v(CN), 2042, 2051, 2061, 2092 cm⁻¹

TBA₂[Ru([H₁₆]-dpb)(CN)₄].2H₂O (**3a**):Yield 35%. Abs 253 nm ($\pi-\pi^*$, ε=27800), 303 nm ($\pi-\pi^*$, ε=23600), 418 nm (MLCT, ε=4500); Corrected emission maximum: 652 nm (298 K); ¹H NMR (D₂O): δ 8.86 (d, 2H), 8.28(s, 2H), 7.82-7.58 (m, 10H) 7.26 (d, 2H) 3.06 (qa, 16H), 1.54 (qi, 16H), 1.27 (sx, 16H), 0.88 (t, 24H); IR v(CN) 2038, 2053, 2067, 2094 cm⁻¹

TBA₂[Ru([D₁₆]-dpb)(CN)₄].2H₂O (**3b**): Yield 20%. Abs 253 nm ($\pi-\pi^*$), 303 nm ($\pi-\pi^*$), 418 nm (MLCT); Corrected emission maximum: 650 nm (298 K); ²H NMR (H₂O, 363 K) 9.77 (2H), 9.03 (2 H), a peak with two maxima at 8.48 (4H), and 8.26 (7.6H); IR v(CN), 2038, 2055, 2066, 2096 cm⁻¹

K₄[Ru(4,4-dcb)(CN)₄] (**4**): Yield 27%. Abs 302 nm ($\pi-\pi^*$, ε=27600), 425 nm (MLCT, ε=6620); Corrected emission maximum: 665 nm (298 K); ¹H NMR (D₂O): δ 9.17 (d, 2H), 8.56 (d, 2H),7.74 (dd, 2H); ¹³C NMR (D₂O) δ 174.7, 167.4, 165.9, 158.5, 155.6, 147.0, 127.9, 123.8; IR v(CN) 2029, 2042, 2058, 2064, 2099 cm⁻¹.

K₂[Ru([D₈]-phen)(CN)₄].2H₂O (**5b**):Yield 23%. Abs 261 nm ($\pi-\pi^*$), 385 nm (MLCT); Corrected emission maximum: 610 nm (298 K); ¹H NMR (D₂O): δ 9.45 (s, 2H), 8.22 (s, 2H), 7.72 (s, 2H), 7.51 (s, 2H); ²H NMR δ 9.43 (2H), 8.325 (2H), 7.758 (4H); IR v(CN) 2041, 2050, 2060, 2093 cm⁻¹

K₂[Ru(2,9-dmphen)(CN)₄] (**6**): Yield 8%. Abs 264 nm ($\pi-\pi^*$, ε=29900), 363 nm (MLCT, ε=4520); Corrected emission maximum: 606 nm (298 K); ¹H NMR (D₂O): δ 8.00 (d, 2H), 7.49 (d,2H), 7.35 (s, 2H) 3.27 (s, 6H); IR v(CN) 2022, 2045, 2061, 2079, 2096 cm⁻¹.

K₂[Ru(4,7-dmphen)(CN)₄] (**7**): Yield 35%. Abs 260 nm ($\pi-\pi^*$, ε=46900), 380 nm (MLCT, ε=6780); Corrected emission maximum: 605 nm (298 K); ¹H NMR (D₂O): δ 9.22 (d, 2H), 7.50 (d,2H), 7.29 (s, 2H) 2.23 (s, 6H); IR v(CN) 2042, 2051, 2061, 2064, 2096 cm⁻¹.

$K_2[Ru(5,6-dmphen)(CN)_4]$ (**8**): Yield 20%. Abs 266 nm ($\pi-\pi^*$, $\epsilon=38960$), 380 nm (MLCT, $\epsilon=5600$); Corrected emission maximum: 610 nm (298 K); 1H NMR (D_2O): δ 9.40 (d, 2H), 8.34 (d, 2H), 7.72 (dd, 2H) 2.02 (s, 6H); IR v(CN) 2038, 2054, 2067, 2093 cm^{-1} .

$K_2[Ru([H_{16}]-ph_2phen)(CN)_4].2H_2O$ (**9a**): Yield 48%. Abs 272 nm ($\pi-\pi^*$, $\epsilon=54000$), 396 nm (MLCT, $\epsilon=10500$); Corrected emission maximum: 647 nm (298 K); 1H NMR (D_2O): δ 9.57 (d, 2H), 7.65 (d, 2H) 7.25 (s, 2H), 7.05-6.8 (m, 10H); IR v(CN) 2039, 2056, 2068, 2096 cm^{-1}

TBA₂[Ru([D₂]-ph₂phen)(CN)₄]₂H₂O (**9b**): Yield 48%. Abs 272 nm ($\pi-\pi^*$), 396 nm (MLCT); Corrected emission maximum: 647 nm (298 K); 1H NMR (D_2O): δ 7.58 (s, 2H) 7.27 (s, 2H), 7.09-6.84 (m, 10H), 2.96 (qa, 16H), 1.43 (qi, 16H), 1.16 (sx, 16H), 0.746 (t, 24H); 2H NMR (H_2O , 358 K) δ 10.1, IR v(CN) 2040, 2058, 2062, 2093 cm^{-1} .

TBA₂[Ru([D₁₂]- ph₂phen)(CN)₄]₂H₂O (**9c**): Yield 54%. Abs 272 nm ($\pi-\pi^*$), 396 nm MLCT); Corrected emission maximum: 647 nm (298 K); 1H NMR (D_2O): δ 9.48 (s, 2H), 7.31 (s, 1.6H), 7.06 (s, 1.8H); 2H NMR (H_2O , 358 K) δ , broad band 8.06 with a shoulder at 8.27; IR v(CN) 2042, 2063 (broad band), 2094 cm^{-1} .

$K_2[Ru([D_{12}]- ph_2phen)(CN)_4].2H_2O$ (**9d**): Yield 28 %. Abs 272 nm ($\pi-\pi^*$), 396 nm (MLCT); Corrected emission maximum: 647 nm (298 K); 1H NMR (D_2O): δ 9.57 (s, 0.2H), 7.27 (s, 2H), 7.05 (s, 0.2H), 6.91 (s, 0.2H); 2H NMR (H_2O , 363 K) δ 10.13 (2H), 7.96 with a shoulder at 8.37 (12.4 H); IR v(CN) 2040, 2053, 2065, 2092 cm^{-1} .

$K_2[Ru([D_{16}]- ph_2phen)(CN)_4].2H_2O$ (**9e**): Yield 30%. Abs 272 nm ($\pi-\pi^*$), 396 nm (MLCT); Corrected emission maximum: 647 nm (298 K); 2H NMR (H_2O , 358 K) δ 10.08 (2H) 7.87 with a shoulder at 8.17 ppm (14 H); IR v(CN) 2040, 2053, 2064, 2093 cm^{-1} .

¹H NMR and photophysical Data.

Table S1. 1H NMR shift of protons in different position of phenanthroline skeleton of $[Ru(LL)(CN)_4]^{2-}$.

LL	1H NMR shift (ppm) of protons				
	2.9	3.8	4.7	5.6	methyl
phen	9.38	8.25	7.70	7.62	-
5,6-dmphen	9.40	8.30	7.72	-	2.02
4,7-dmphen	9.22	7.50	-	7.29	2.32
2,9-dmphen	-	8.00	7.49	7.35	3.27
4,7-dpphen	9.57	7.65	-	7.25	

Table S2. Fitting parameters of emission spectra measured at 77 K in ethanol/methanol glass.

	E_{00} (cm^{-1})	S_M	$h\omega_M$ (cm^{-1})	$\Delta\nu_{2/1}$ (cm^{-1})
1a	17522	1.01	1300	1260
2a	17837	1.1	1300	1323
3a	16952	0.77	1320	1250
4	16526	0.79	1320	1250
5	17500	0.82	1300	1220
6	18100	0.92	1300	1310
7	18190	1.05	1300	1270
8	17910	0.85	1320	1280
9a	16825	0.73	1290	1260
9e	16868	0.74	1290	1270

^a The confidence interval of the fitted parameters is not higher than 1 %

Table S3. Lifetime of the excited $[\text{Ru(LL)(CN)}_4]^{2-}$ complexes (77 K in ethanol/methanol 4/1 glass and 298 K using Ar saturated aqueous solutions of complexes) and the luminescence quantum yield (298 K in Ar saturated H_2O).

	$\tau_{77\text{K}} (\mu\text{s})$	$\tau_{298\text{K}} (\text{ns})$	Φ_{ph}
1a	2.9	120	0.0076
1b	3.1	132	0.0084
2a	2.8	113	0.0073
2b	3.2	124	0.0081
3a	3.4	145	0.0105
3b	3.6	156	0.0111
4	-	100	0.0053
5a	9.5	590	0.025
5b	9.9	654	0.0315
6	-	570	0.0439
7	-	1209	0.0432
8	-	560	0.0305
9a	10.8	838	0.0213
9b	10.2	874	0.021
9c	11.9	902	0.0206
9d	11.6	954	0.023
9e	12.7	960	0.022

Table S4 Photophysical parameters estimated by fitting procedure used equation (1).

	$k_{\text{ph}} \times 10^{-4} (\text{s}^{-1})$	$k_{\text{nr}} \times 10^{-5} (\text{s}^{-1})$	$A \times 10^{-8} (\text{s}^{-1})$	$\Delta E (\text{cm}^{-1})$
1a	6.3	44	15.7	1245
1b	6.4	35	10	1150
2a	6.5	44	15.8	1220
2b	6.5	38	7.3	1080
3a	7.2	20	7.3	1050
3b	7.1	4.5	3.6	855
4	5.7	53	5.4	972
5a	4.2	8.4	7.7	1400
5b	4.8	6.9	4.5	1315
6	7.7	5.6	12.3	1455
7	3.6	3.2	5.7	1480
8	5.4	9.7	12.7	1540
9a	2.50	5.05	7.3	1447
9b	2.38	4.5	5.4	1407
9c	2.28	-	-	-
9d	2.40	-	-	-
9e	2.33	4.7	7.14	1488

Table S5. Rate coefficients and activation parameters of photophysical deactivation processes in H₂O, estimated by 3 data sets with 7 parameters.

	complex	$k_{ph} \times 10^{-4}$ (s ⁻¹)	$k_{nr} \times 10^{-5}$ (s ⁻¹)	$A \times 10^8$ (s ⁻¹)	ΔE (cm ⁻¹)
1a		6.3±0.3	41.3±1.3	10.3±1.80	1140±40
^a 1a		7.6±0.3	10.5±0.5	4.02±0.69	1140±40
1b		6.4±0.4	35.7±1.1	9.55±1.65	1140±40
2a		6.5±0.3	45.0±1.5	15.8±2.6	1220±40
^a 2a		6.8±0.4	10.9±0.6	6.29±1.08	1220±40
2b		6.5±0.3	43.4±1.2	12.7±2.2	1220±40
3a		7.2±0.5	16.8±1.6	5.52±0.64	970±30
^a 3a		7.6±0.5	2.77±0.62	2.09±0.24	970±30
3b		7.1±0.5	14.1±1.6	5.47±0.63	970±30
5a		4.2±0.2	8.93±0.30	6.89±1.17	1408±40
^a 5a		5.7±0.3	2.40±0.09	2.44±0.42	1408±40
5b		4.8±0.3	7.92±0.25	6.54±1.13	1408±40
9a		2.5±0.1	5.07±0.22	6.25±1.03	1408±40
9b		2.4±0.1	5.09±0.20	5.46±0.90	1408±40
9e		2.3±0.1	4.61±0.18	5.19±0.85	1408±40

^ameasured in D₂O

Table S6. Rate coefficients and activation parameters of photophysical deactivation processes, estimated by 11 parameters and using 3 data sets.

Solvent	$k_{ph} \times 10^{-4}$ (s ⁻¹)	$k_{nr} \times 10^{-5}$ (s ⁻¹)	$A_{4th} \times 10^{-7}$ (s ⁻¹)	ΔE_{4th} (cm ⁻¹)	$A_{dd} \times 10^{-12}$ (s ⁻¹)	ΔE_{dd} (cm ⁻¹)
1a	CH ₃ OH	3.6±0.3	60.4	45	790	150
	CH ₃ OD	3.6±0.3	35.0	25	788	150
	CD ₃ OD	3.7±0.4	33.8	26	791	150
5a	H ₂ O	4.2±0.2	4.17	5.17	780	0.99
	D ₂ O	5.7±0.3	0.56	1.72	780	0.42
5b	H ₂ O	4.8±0.3	3.19	4.93	780	0.94
9a	H ₂ O	2.5±0.1	1.75	2.12	663	2.21x10 ⁻²
9b	H ₂ O	2.4±0.1	1.30	2.14	663	1.64x10 ⁻²
9e	H ₂ O	2.3±0.1	0.50	2.19	663	1.40x10 ⁻³

Resonance Raman and transient absorption spectroscopy

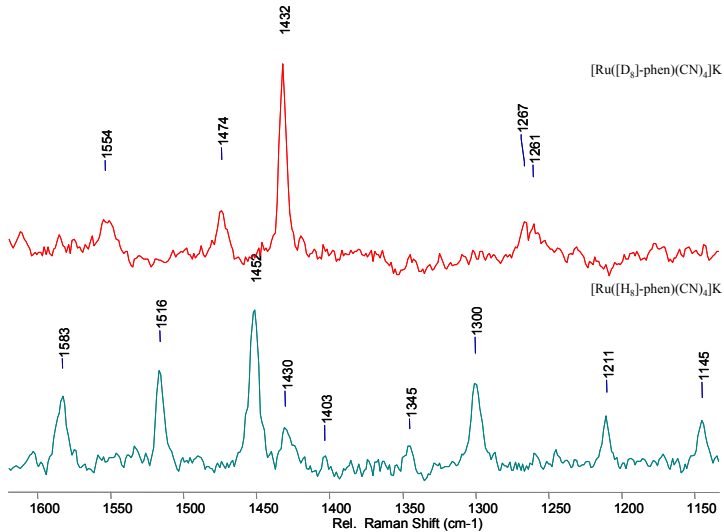


Fig. S1. Ground state resonance Raman (in H₂O, $\lambda_{\text{ex}}=457.9$ nm) of **5a** (lower) and **5b** (upper).

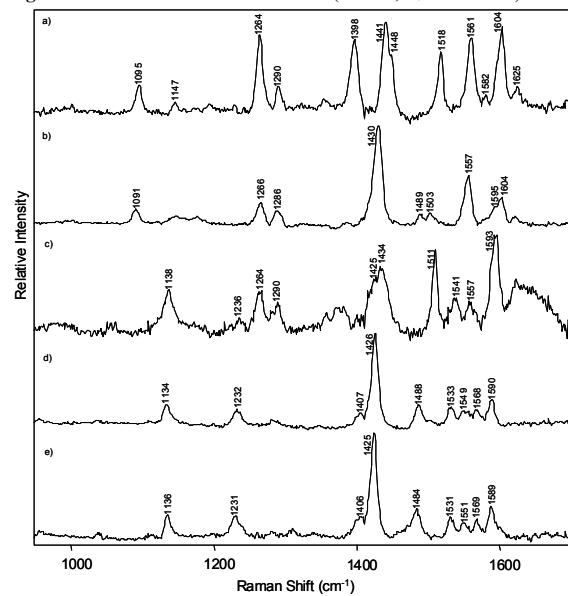


Fig. S2. Ground state resonance Raman spectra for (in H₂O, $\lambda_{\text{ex}}=457.9$ nm) a) **9a**; b) **9b**; c) **9c**; d) **9d**; e) **9e**.

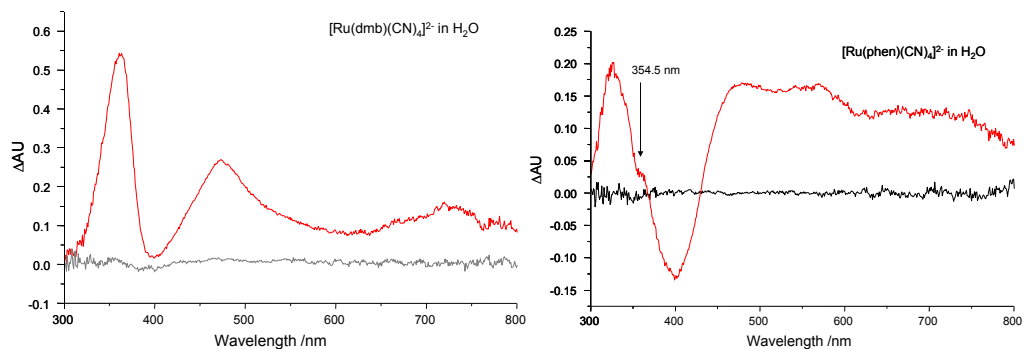


Fig. S3 The transient absorption spectrum of left: **2a**, and right: **5a** in H₂O detected by excitation of a laser pulse ($\lambda_{\text{exc}} = 354.5$ nm, with a 10 ns delay).

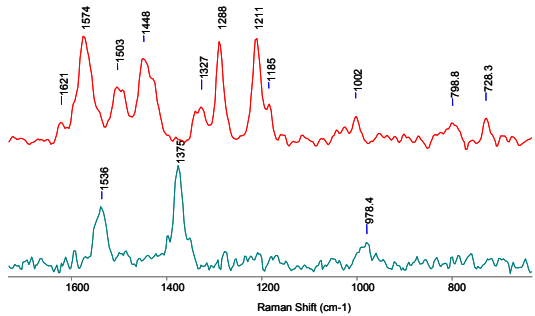


Fig. S4 TR² spectra of **2a** (red) and **2b** (green) in H₂O, λ_{exc} 354.67 nm.

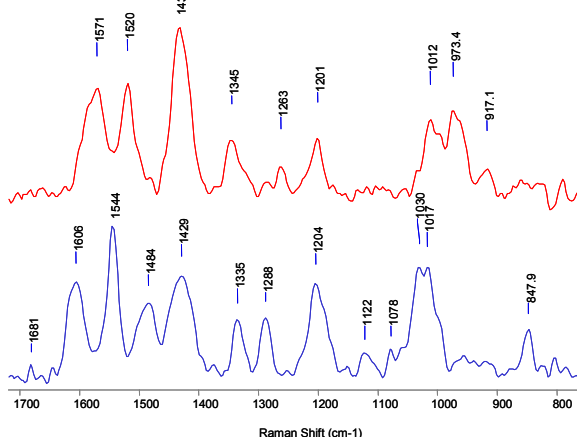


Fig. S5 TR² spectra of **3a** (blue) and **3b** (red) in H₂O, λ_{exc} 354.67 nm.

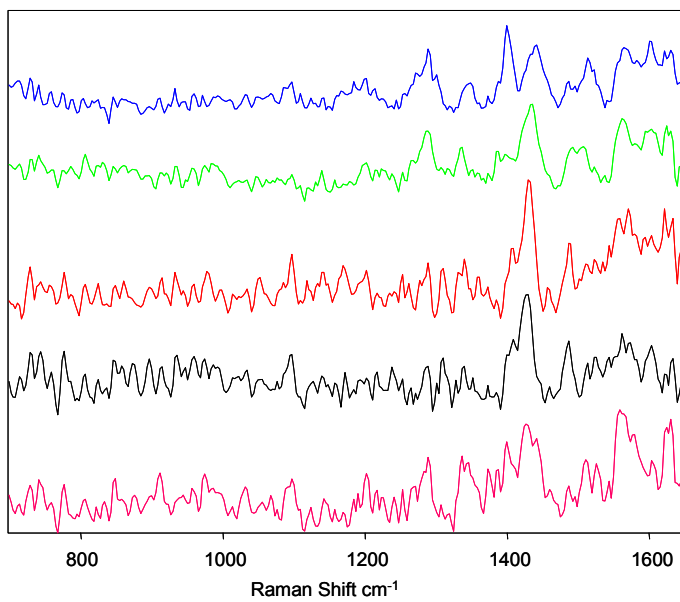


Fig. S6 TR² spectra of (top to bottom) **9a-9e** in H₂O, λ_{exc} 354.67 nm.